Numerical and experimental study on efficacy of layered foundation in reduction of railway-induced vibrations

Javad Sadeghi[1], Ehsan Haghighi and Nima Hadadi

School of Railway Engineering, Iran University of Science and Technology, Tehran, Iran

Abstract. This paper investigates the effectiveness of layered foundation systems in mitigating railway-induced vibrations using a Finite Element/Infinite Element (FE/IE) model and a scaled-down laboratory model. Traditional single-layer isolators often face bearing capacity limitations, prompting the use of layered under-foundation isolators (LUFI) as a practical alternative. Five different isolator configurations, including single-layer (SUFI) and multi-layer (LUFI) setups, were assessed under varying soil conditions and building characteristics. The study employed a parametric analysis to evaluate vibration reduction performance, measured by the Insertion Loss (IL) index. Results indicate that single-layer isolators generally outperform multi-layer isolators of equivalent total thickness, particularly in stiffer soil conditions. However, when the rubber thickness is increased proportionally across multiple layers, multi-layer isolators demonstrate superior vibration attenuation. The effectiveness of the proposed isolation method in a real-world situation was then confirmed by developing a 3D numerical model and a scaled-down laboratory model of a building adjacent to a railway track. The accuracy of the numerical approach was also validated by comparing its results with those from the laboratory model. The study underscores the importance of considering soil-structure interaction, isolation frequency, and isolation layers in the design of effective vibration mitigation systems.

Keywords: railway-induced vibrations; layered foundation; isolation performance; numerical modeling; laboratory model

1 **Corresponding Author, Professor, E-mail:** Javad_Sadeghi@rail.iust.ac.ir

1. Introduction

Urban environments are increasingly challenged by ground-borne vibrations, particularly those induced by train traffic (Hanson et al., 2006; Khajehdezfuly et al., 2023; Standard and ISO, 2005). As railway networks expand, the impact of these vibrations on buildings and their occupants becomes a significant concern. Ground-borne vibrations, propagating as elastic waves through the soil, can cause discomfort to inhabitants, damage to sensitive and historic structures, and disruption to equipment in facilities like hospitals and laboratories (Farahani et al., 2023; Sadeghi et al., 2023; Sadeghi and Esmaeili, 2017; Sadeghi and Vasheghani, 2021, 2022; Standard, 1989). Addressing these challenges requires innovative solutions that can effectively mitigate vibrations and protect urban infrastructure.

Traditional methods for mitigating train-induced vibrations include track modifications, soil treatments, and building isolation techniques. Track modifications, such as resilient rail fasteners and under-sleeper pads, aim to reduce vibrations at the source (Lei and Jiang, 2016; Li et al., 2019; Sadeghi et al., 2024; Sol-Sánchez et al., 2015; Yuan et al., 2020; Zhao et al., 2022). However, these solutions often have limitations, including effectiveness at specific frequencies and potential adverse effects on track performance. Soil treatments and barriers, such as trenches and wave-impeding blocks, attempt to block or attenuate vibrations in the transmission path (Celebi and Göktepe, 2012; Pu and Shi, 2020; Ribes-Llario et al., 2017; Toygar and Ulgen, 2021; Zhou et al., 2022). While effective, these methods can be impractical in dense urban areas due to space constraints and high costs.

Building isolation techniques have gained popularity as a means to decouple structures from ground vibrations. This method involves placing isolators such as rubber bearings (Talbot, 2007) between a building and its foundation or a resilient layer (Sadeghi et al., 2021) between the foundations and the ground. These isolators absorb and dissipate energy, reducing the amplitude of vibrations transmitted to the structure. Elastic bearings have been widely used in the isolation of buildings against ground-borne vibrations since the 1960s (Newland and Hunt, 1991). These bearings, typically made of rubber or similar resilient materials, act as shock absorbers that decouple the building from ground motion (Kelly and Konstantinidis, 2011; Newland, 2013). The efficiency of elastic bearings has been thoroughly examined in several analytical (Newland, 2013), numerical (Soares et al., 2024; T. L. Edirisinghe and J. P. Talbot, 2022; Talbot et al., 2014; J Yang et al., 2019), and experimental (Pan et al., 2018; Sheng et al., 2020; Soares et al., 2024) studies. While elastic

bearings are effective, they can be expensive and require precise installation to achieve the desired performance. An alternative and innovative approach to vibration isolation is the implementation of resilient layers beneath the foundation. This method is practical and cost-effective compared to elastic bearings and has been shown to be efficacious in mitigating ground-borne vibrations (Haghighi et al., 2023, 2024; Sadeghi et al., 2021, 2022). Recent numerical and experimental research by (Haghighi et al., 2023, 2024; Sadeghi et al., 2021, 2022) demonstrated the effectiveness of this method, highlighting its potential as a practical solution for urban environments.

Despite the proven efficiency of under-foundation layers in reducing railway vibrations, their implementation is sometimes constrained by the bearing capacity limitations of the rubber mat (Isolgomma, 2024). In such cases, a single thick isolation layer may not be feasible. To overcome this challenge, the required thickness for effective isolation can be divided into several thinner layers, creating a layered foundation. Implementing layered structures, originally developed for seismic isolation (Cheng et al., 2020), offers a promising new approach to mitigating train-induced vibrations. These layered structures have also recently been used as layered wave barriers to mitigate traffic-induced vibrations (Pu et al., 2018; Pu and Shi, 2020). The application of layered structures as layered foundations for seismic isolation and as wave barriers for mitigating traffic-induced vibrations is schematically illustrated in Figure 1. As observed, these kinds of isolators are composed of alternating layers of materials with different elastic properties, such as concrete and rubber. Therefore, this approach not only enhances the bearing capacity of the under-foundation rubber mat but also maintains the vibration isolation effectiveness.

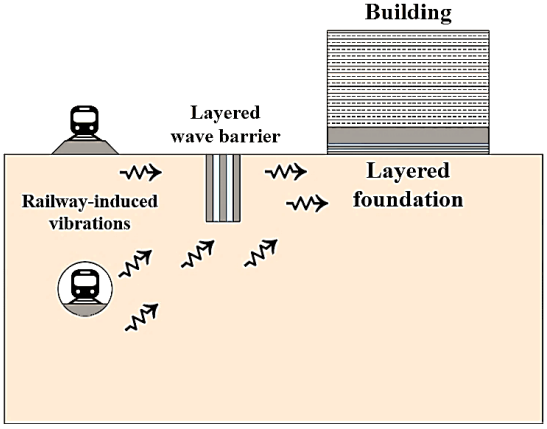

Figure 1. Schematic view of layered foundations and layered wave barriers (adopt from Cheng et al., 2020).

This paper encompasses a blend of numerical and experimental modeling analysis to investigate the efficacy of layered foundations in mitigating railway-induced vibrations, a novel approach that extends their proven effectiveness in seismic isolation to a new domain. To this end, initially, a 2D finite element model was developed to simulate the dynamic behavior of soil-structure interaction under railway loading conditions. Various configurations of Single Under Foundation Isolators (SUFI) and Layered Under Foundation Isolators (LUFI) were analyzed to assess their performance against train-induced vibration. The numerical models considered parameters such as isolation frequency, soil stiffness, building's floor natural frequency, and the number and thickness of isolator layers. Additionally, a detailed laboratory study was conducted on a five-story concrete building near a railway line to confirm the effectiveness of layered foundations in a real-world situation and validate the numerical modeling approach employed in this research. The combined approach of numerical and physical simulations of a real-world problem provided a robust framework to evaluate the performance of different isolation strategies and their practical implications.

2. Model description

Assessing vibrations caused by railways in nearby buildings poses a complex 3D soil-structure interaction challenge. Nevertheless, when assessing the effectiveness of vibration reduction systems by comparing dynamic responses in isolated and unisolated scenarios, 2D models demonstrate reliability and cost-effectiveness for conducting parametric analyses (Haghighi et al., 2023; Sadeghi et al., 2021, 2022). Additionally, it is common practice to use a simplified frame model to represent a complex building when evaluating vibration levels near railway tracks. (Sadeghi et al., 2021; Yang et al., 2017; Yang and Hung, 2009). This approach facilitates more in-depth discussions based on the study results. In this context, a 2D Finite Element/Infinite Element (FE/IE) plane-strain numerical model has been established using ABAQUS (Dassault Systèmes, 2014) to evaluate the dynamic response of an isolated building with Singular Under Foundation Isolator (SUFI) and Layered Under Foundation Isolators (LUFI).

2.1. Geometrical dimensions and model meshing

Figure 2a illustrates the conceptual model comprising a single-story concrete building with a foundation, vibration isolators (SUFI and LUFI), and a surrounding soil medium. Detailed in Figure 2b, the building features two columns (0.25 m × 3.6 m) connected by a beam (5.5 m × 0.25 m), all resting on a foundation (6 m × 0.4 m). The simulation utilized the 4-node plane strain element of CPE4 for these components, while the infinite element of CINPE4 was utilized at the model boundaries to prevent wave reflection, ensuring that the finite domain dimensions did not affect the results. To ensure adequate space, the finite domain was established at 60 meters wide and 40 meters deep. Considering the softest soil's properties, it was established that the mesh element size should not exceed one-fifth of the Rayleigh wavelength (Xu et al., 2015; Zhang et al., 2019); thus, element dimensions were kept under 0.5 m.

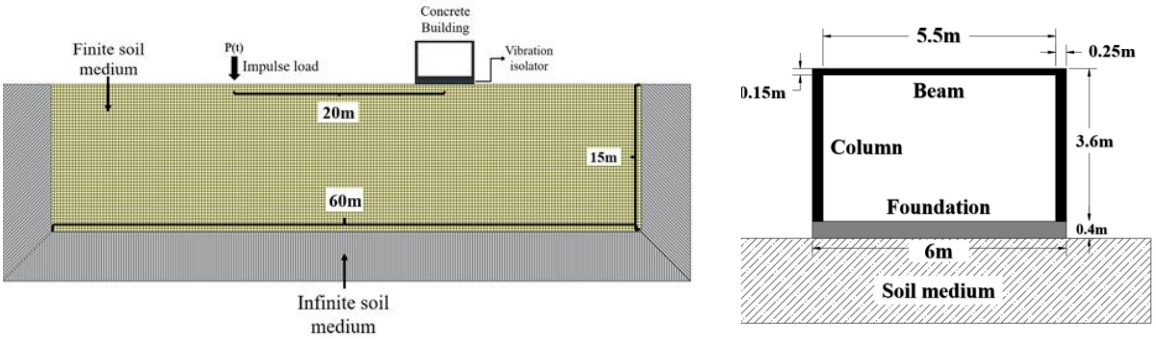

(a) whole model (b) unisolated frame

Fig 2. Details of the 2D numerical model

2.2. Building isolation assumptions and methods

To investigate the performance of layered foundations, five different configurations were considered in the parametric study, as shown in Figure 3. These configurations aim to evaluate how varying the number of layers and overall thickness affects the foundation's performance. The first type is a single-layer isolator with a rubber thickness of t equal to 0.2m, referred to as SUFI-t. The second type includes two-layer and four-layer isolators, each with a total rubber thickness of 0.2m, denoted as 2LUFI-t and 4LUFI-t, respectively, with 0.1m-thick concrete layers between them. Therefore, the two-layer and four-layer models achieve total thicknesses of 0.3m and 0.5m,

respectively. The third isolator type consists of two-layer and four-layer isolators with total rubber thicknesses of 0.4m and 0.8m, referred to as 2LUFI-2t and 4LUFI-4t, respectively, also interspersed with 0.1m-thick concrete layers. Notably, the total thicknesses of these two-layer and four-layer models are 0.5m and 1.1m, respectively.

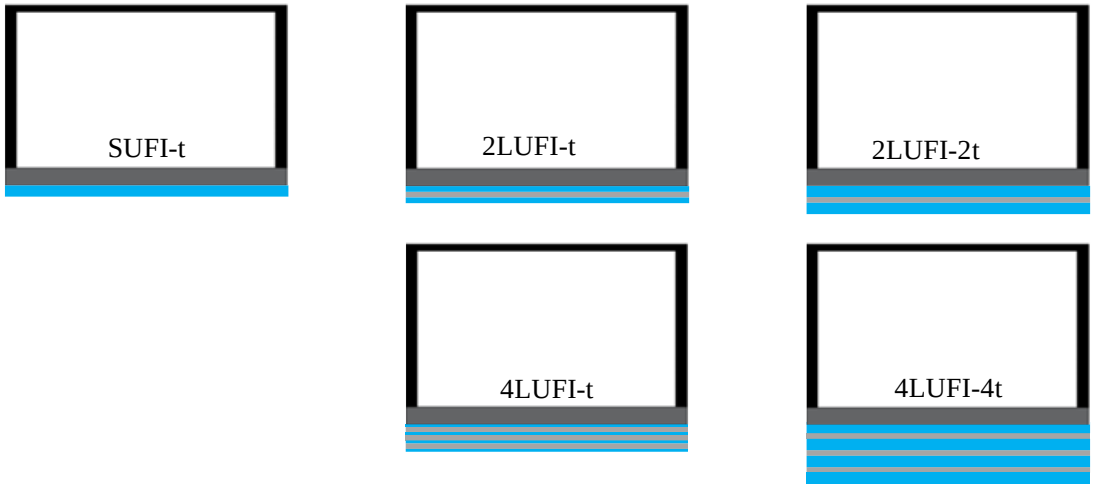

(a) isolation with a single-layer isolator of t thick rubber

(b) isolation with layered isolators having a total rubber thickness of t

(c) isolation with layered isolators where each layer has a rubber thickness of t.

Figure 3. Building isolation with different types of isolators

2.3. Simulating train load

To evaluate the performance of under-foundation isolators, a simplified simulation was conducted to replicate the dynamic loads generated by train movements. The interaction between train wheels and rails induces vibrations that propagate through the surrounding environment in both vertical and horizontal directions. These vibrations typically are less than 80Hz, annoying for building residents (Sadeghi et al., 2021; Standard, 2010; Zhang et al., 2021). To simulate these vibrations accurately, an impulse load of 150kN was exerted at a distance of 20 meters from the center of the building. This impulse load is defined by the function (Kouroussis et al., 2013; Sadeghi et al., 2021):

$$P(t) = \begin{cases} 0 & , \quad t < t0 \\ P_0 e^{\left(\frac{-(t-t_0)}{t_d}\right)}, & t \geq t0 \end{cases} \quad (1)$$

In this equation, P_0 represents the load amplitude, t_0 signifies the time delay, and t_d denotes the load duration. The parameters chosen for this study were P_0=1N, t_0 = 0.02s and t_d = 0.00125s, ensuring the simulation accurately captures the frequency characteristics up to 80Hz. Figure 4 provides a graphical representation of this impulse load in both the time and frequency domains, illustrating how the applied load effectively stimulates the desired frequency range for assessing the structural response.

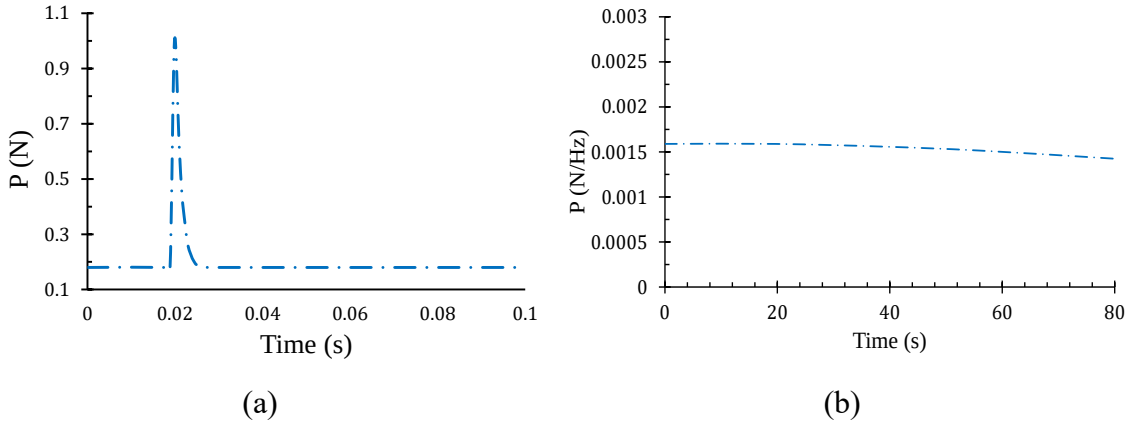

Fig 4. Impulse loading, (a) time history and (b) frequency content

2.4. Properties of materials in the parametric analysis

A detailed parametric study was conducted to assess the impact of building characteristics, isolator properties, and soil media on the efficiency of SUFIs and LUFIs in mitigating railway-induced vibrations.

To investigate the effect of soil type on the efficiency of the isolators, four soil types including soft (S1), medium (S2), stiff (S3), and high-dense (S4) were selected based on international codes (Engineers, 2010). These soils were chosen to cover a realistic range of conditions encountered in practice. In numerical modeling, the Yang modulus is a crucial parameter required to characterize the soil properties, which can be calculated by (Towhata, 2008):

$$E_s = 2\rho(1+v){V_s}^2 \quad (2)$$

in which V_s is the shear wave velocity of the soil media, E_s is the elastic modulus of the soil, ρ is the soil density and ν is the soil Poisson's ratio. Additionally, the soil damping ratio, which is approximately 2% for small strains (Mousavi-Rahimi et al., 2022; Towhata, 2008), is also required. The specifications of selected soil types are detailed in Table 1.

Table 1. Specifications of soil types in parametric analysis (partially adapted from Haghighi et al., 2023)

Soil type	Density	modulus of elasticity	Poisson's ratio	Shear wave velocity	Damping ratio
	ρ (kg/m^3)	E_s (MPa)	ν (-)	V_s (m/s)	ξ (%)
S1 (soft)	1750	100	0.33	147	2
S2 (medium)	1750	200	0.33	207	2
S3 (stiff)	1750	400	0.33	293	2
S4 (high dense)	1750	800	0.33	415	2

The dynamic response of a building to ground-borne vibrations is critically influenced by the natural frequency of its floors, which can be precisely determined through numerical analysis. This frequency typically ranges from 7 to 25 Hz (Bachmann and Ammann, 1987; Zakeri et al., 2020). To conduct a comprehensive parametric analysis, four types of buildings, designated as B1 to B4, were considered, each incorporating floors with varying elastic modulus values. Based on the previous research (Haghighi et al., 2023; Mousavi-Rahimi et al., 2022), the buildings' floor were specifically designed to ensure that their natural frequencies fall within the desired range of 7 to 25 Hz range. The detailed properties of the buildings, including the characteristics of their floors, foundation, and walls, are summarized in Table 2.

Table 2. Properties of buildings in the parametric analysis (partially adapted from Haghighi et al., 2023)

Building name	Component	Mass density	Natural frequency of floor	Modulus of elasticity	Poisson's ratio	Damping ratio
		ρ (kg/m^3)	f_n (Hz)	E (GPa)	ν (-)	ξ (%)
B1	Floor	2500	8	10	0.2	2

B2	Floor	2500	12	30	0.2	2
B3	Floor	2500	18	90	0.2	2
B4	Floor	2500	24	270	0.2	2
B1-B4	Foundation & Walls	2500	-	30	0.2	2

The performance of an isolation systems highly dependent on its isolation frequency (Talbot, 2007). The isolation frequency can be calculated with the following equation (Talbot, 2007):

$$f_{iso} = \frac{1}{2\pi}\sqrt{\frac{E_i \times A}{t_i \times m_{st}}} \quad (3)$$

where E_i and t_i are the elastic modulus and the total thickness of the isolator, m_{st} is the total mass of the building, and A is the total area of foundations. In general, the isolation frequency should be kept significantly lower than the natural frequency of the floor to maximize the effectiveness of isolation systems (Haghighi et al., 2023; Sadeghi et al., 2021, 2022). To this end, four types of rubber mats (named M1 to M4) with a thickness of 0.2m were considered to be utilized as SUFI or LUFI in the parametric study. Details of the isolators and their corresponding isolation frequencies are provided in Table 3.

Table 3. Characteristics of rubber mats in parametric study.

Rubber mat	**Mass density**	**Elastic modulus**	**Isolation frequency**
	ρ **(kg/m^3)**	E_i ***(kPa)***	f_{iso} **(Hz)**
M1	700	150	3
M2	700	415	5
M3	700	810	7
M4	700	2400	12

3. Parametric analysis on the 2D model

As stated in the previous section, soil stiffness, the natural frequency of the floor and the isolation frequency influence the dynamic response of the isolated building. In this research, the

performance of SUFIs and LUFIs in mitigation railway-induced vibrations is evaluated in both horizontal and vertical directions. To evaluate efficiency of isolation systems, the dynamic responses of the floor's midpoint was measured. The index of Insertion Loss which can be calculated as below (Talbot, 2002) was used to assess the efficiency of SUFIs and LUFIs:

$$IL = -20 \times Log_{10}\left(\frac{v_{iso}}{v_{uniso}}\right) \quad (4)$$

where v_{iso} and v_{unsio} are the roots mean square (RMS) velocity amplitudes in the states where the building is isolated and unisolated. The value of insertion loss index indicates the ability of the isolator in vibration mitigation. More precisely, the higher the values obtained for this index, the better the isolator performs in reduction the vibration level. It should be noted that the values calculated from Equation 4 can be negative. The negativity of the index actually highlights the reverse performance of the isolator. In other words, the isolator in such cases not only is unable decrease vibrations, but also leads to increasing it. Therefore, similar to previous studies (Haghighi et al., 2023; Sadeghi et al., 2021; Talbot, 2002), it can be inferred that layered isolators do not always mitigate the vibration level.

To achieve the research objectives, a parametric analysis was conducted across two distinct scenarios. In the first scenario, the performance of single-layer isolators with a rubber thickness of *t* (SUFI-t) was compared to that of multi-layer isolators, each with a total rubber thickness of *t* (2LUFI-t and 4LUF-t). In the second scenario, the performance of SUFI-t was compared to that of multi-layer isolators where each individual layer had a rubber thickness of *t* (2LUFI-2t and 4LUFI-4t). This comparative analysis allowed for a comprehensive evaluation of isolator performance across different structural configurations.

3.1. Results of the first scenario (SUFI-t, 2LUFI-t, and 4LUFI-t)

The curves of insertion loss index for various types of isolators, when the thickness of rubber mats in all types is equal against shear wave velocity of soil under B1 to B4 in horizontal and vertical directions, are illustrated in Figures 5 and 6.

As illustrated, increasing the frequency of isolation from 3 Hz to 12 Hz for all isolator types results in a noticeable decrease in isolation efficiency, with an average reduction of about 20 dB in

both horizontal and vertical directions. This demonstrates that lower isolation frequencies are more effective in mitigating vibrations. The trend suggests that as the isolation frequency increases, the ability of the isolator to dampen vibrations diminishes, likely due to the reduced flexibility of the isolator at higher frequencies.

The stiffness of the beneath soil, characterized by the shear wave speed of soil, significantly impacts the isolators' performance. As soil stiffness increases (from 130 m/s to 390 m/s), the insertion loss improves, indicating better isolation efficiency. This trend underscores the importance of considering soil conditions in the design of vibration isolation systems. Stiffer soils enhance the effectiveness of isolators by providing a more stable base, which better supports the isolation system. The frequency of first mode in the building's floor also plays a crucial role in the effectiveness of the isolators. The figures suggest that buildings with higher natural frequencies (B3 and B4) exhibit different trends in isolation efficiency compared to those with lower natural frequencies (B1 and B2). For instance, in B4, the efficiency initially decreases before improving in the horizontal direction, whereas in B1, a consistent increase in efficiency is observed. This indicates that the interaction between soil and structure is crucial in determining the performance of vibration isolators. The efficiency of the isolator can vary significantly (by about 5 dB to 15 dB) with changes in soil shear wave velocity and natural frequency of the floor. This variability highlights the need for a comprehensive understanding of soil-structure interaction effects in the design process. Neglecting these interactions can lead to suboptimal isolator performance, where in some cases, the vibration levels in isolated buildings could exceed those in unisolated buildings.

When comparing different types of isolators, it is evident that single-layer isolators (SUFI-t) outperform multi-layer isolators (2LUFI-t and 4LUFI-t) across most buildings and isolation frequencies. This suggests that when the total thickness of the isolator is constant, a single-layer configuration provides better vibration isolation than a multi-layer configuration. This could be due to the incurrence of internal resonance in SUFI-t compared to the multi-layer isolators, providing more uniform deformation and energy dissipation in the SUFI-t configuration. Nonetheless, this difference is insignificant, and a multi-layered foundation is feasible when the rubber layer's bearing capacity is constrained.

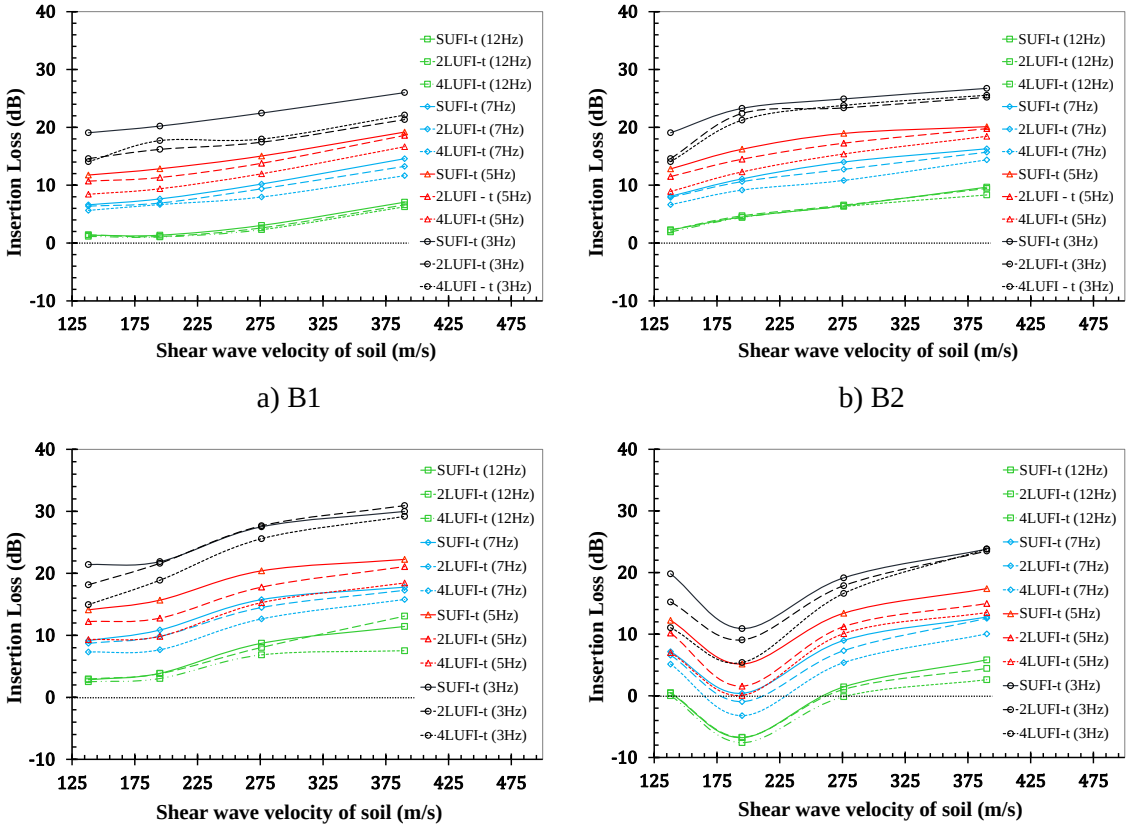

257 **Fig 5**. Insertion loss against shear wave velocity of soil for various isolator types in horizontal direction for
258 the first scenario.
259

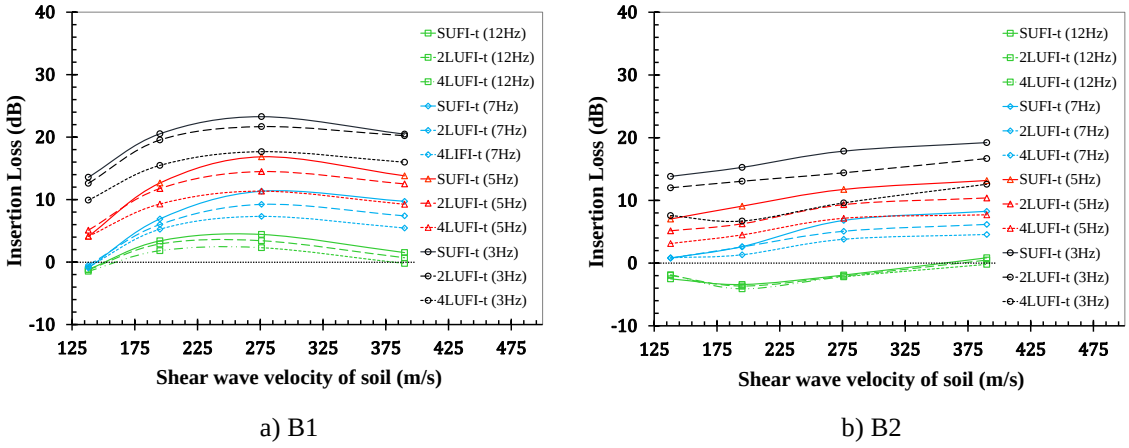

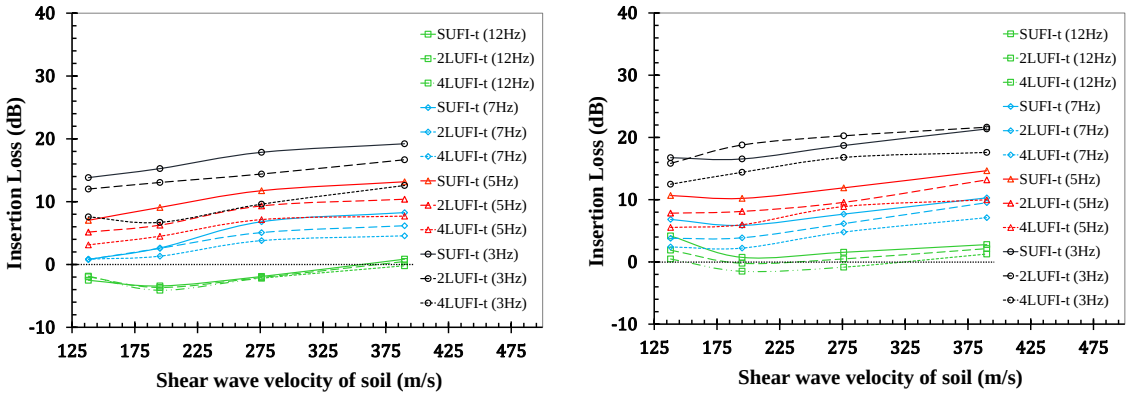

c) B3 d) B4

Fig 6. Insertion loss against shear wave velocity of soil for various isolator types in vertical direction for the first scenario.

3.2. Results of the second scenario (SUFI-t, 2LUFI-2t, and 4LUFI-4t)

Figures 7 and 8 illustrate the curves of the insertion loss index for three types of isolators (SUFI-t, 2LUFI-2t, and 4LUFI-4t). In this scenario, each isolator layer has a rubber thickness of *t* (see Figure 3), and the curves are shown with respect to soil shear wave velocity under conditions B1 to B4, in both horizontal and vertical directions.

Like the first scenario of analysis, increasing the isolation frequency from 3 Hz to 12 Hz decreases isolation efficiency by about 20 dB in both directions, highlighting the effectiveness of lower isolation frequencies in mitigating vibrations. Soil stiffness significantly affects performance, generally with stiffer soils improving insertion loss. The building's natural frequency also influences efficiency, with higher frequencies (B3 and B4) showing varied trends compared to lower ones (B1 and B2). These findings again underscore the importance of considering soil-structure interactions in designing vibration isolation systems to ensure optimal performance of isolators.

Another important finding is that unlike in the first scenario, increasing the number of isolator layers significantly improves performance of isolators. Specifically, the 4LUFI-4t isolator outperforms the 2LUFI-2t isolator, which in turn outperforms the SUFI-t isolator. On average, 4LUFI-4t reduced vibration levels by approximately 3 decibels more than 2LUFI-2t, while 2LUFI-2t achieved about a 3-decibel greater reduction compared to SUFI-t. This trend suggests that adding more layers enhances the isolator's ability to dampen vibrations effectively. The increased number

of layers provides greater flexibility and improved damping capacity, allowing the isolator to better absorb and mitigate vibrational energy. This result highlights the advantage of multi-layered isolators in applications where superior vibration isolation is crucial.

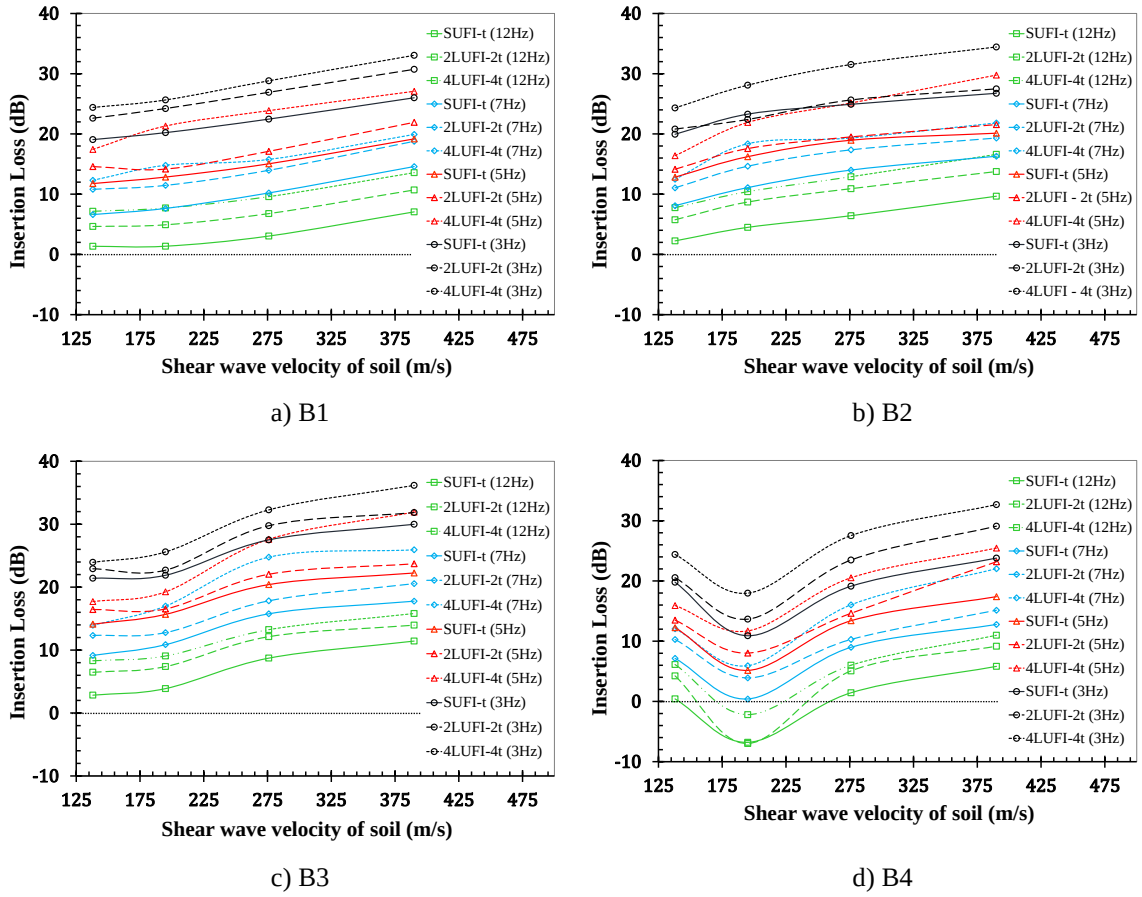

a) B1 b) B2

c) B3 d) B4

Fig 7. Insertion loss against shear wave velocity of soil for various isolator types in horizontal direction for the second scenario.

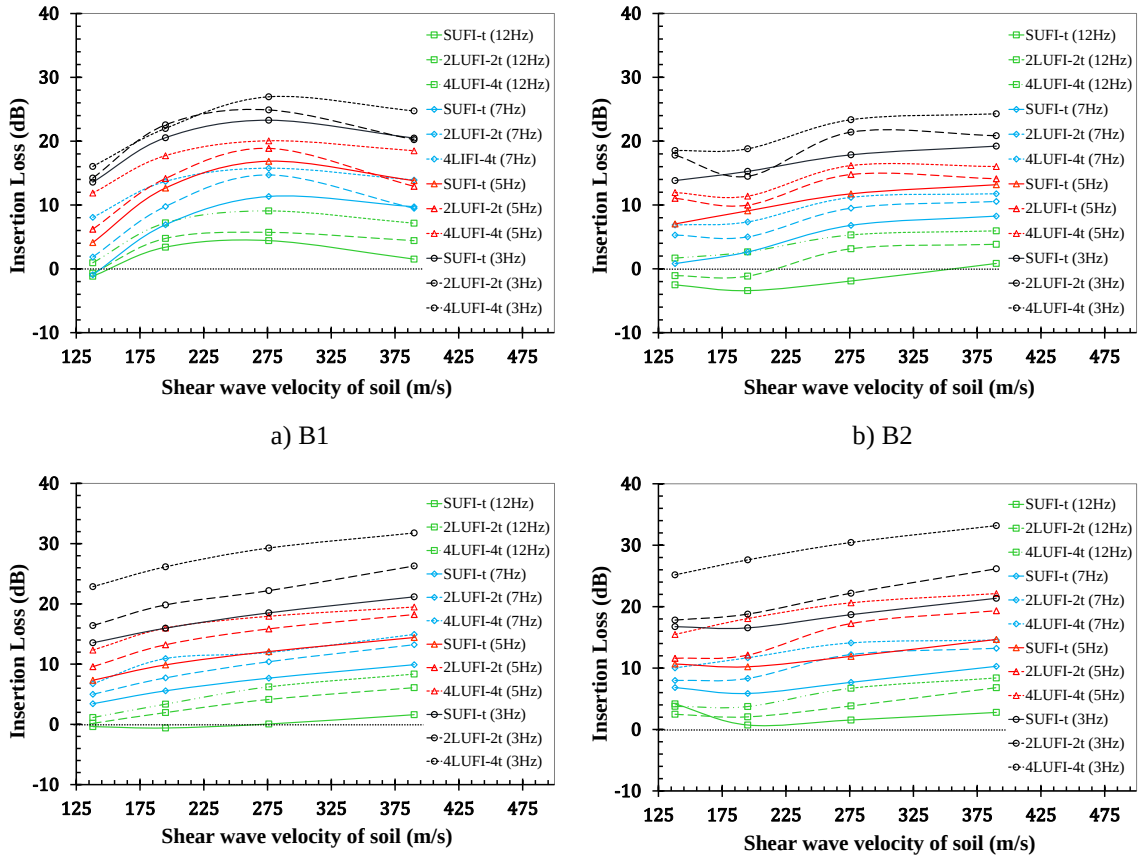

a) B1 b) B2

c) B3 d) B4

Fig 8. Insertion loss against shear wave velocity of soil for various isolator types in vertical direction for the second scenario.

4. Practical evaluation of proposed isolator

While a comprehensive parametric analysis of the 2D numerical model has demonstrated the potential efficacy of the proposed layered foundation as an isolator of ground-borne vibrations, it is imperative to validate these findings in real-world conditions. Conventional buildings generally exhibit natural floor frequencies between 7 and 15 Hz (Bachmann and Ammann, 1987; Zakeri et al., 2020). Considering this range, to assess the effectiveness of the layered foundations in practical applications, we selected a typical five-story concrete building located adjacent to a railway track as a prototype. The selected prototype has been previously examined in the literature for various purposes, such as analyzing the effects of foundation geometry on vibration levels inside the building

300 (Mousavi-Rahimi et al., 2022) and assessing the impacts of soil-structure interaction on the
301 performance of isolators (Haghighi et al., 2023, 2024).
302 The prototype building features four columns placed above four separate foundations. The
303 dimensions of each foundation are 2 meters in length, 2 meters in width, and 1 meter in depth. Each
304 column has a cross-sectional area of 0.5 meters by 0.5 meters and a net height of 3 meters. The slabs
305 measure 6 meters by 6 meters in plane dimensions and had a thickness of 0.15 meters. Thus, the
306 total height of the building from the foundation to the top is 15.75 meters. The material properties
307 of the building include a Young's modulus of 25 GPa, a Poisson's ratio of 0.2, and a density of 2550
308 kg/m³, resulting in a total mass of 148.1 tons. These parameters were essential in constructing an
309 accurate numerical model to simulate the building's response to train-induced vibrations. An impact
310 excitation, represented by Equation 1, was exerted at a distance of 20 meters from the middle of the
311 building. In accordance with the reverse engineering approach, the soil medium was considered with
312 specific properties to satisfy the scale factors in the laboratory model (refer to Section 4.1). It was
313 assumed that the soil had a density of 1630 kg/m³, a shear wave velocity of 590 m/s, and that the
314 bedrock was located 14 meters below the surface. These assumptions were critical in ensuring the
315 accuracy and relevance of soil medium in the physical and numerical models.
316 The isolation strategy for the building involved two parts. In the first part, single resilient
317 layers with a thickness of 9 cm and an elastic modulus of 400 kPa were inserted beneath the building
318 foundation. In the second part, these resilient layers were replaced with a three-layer foundation,
319 where each rubber mat utilized had a thickness of 3 cm. These two scenarios allow for analyzing the
320 effectiveness of single resilient layers versus layered foundations in mitigating ground-born
321 vibrations. The isolation frequency for these isolators can be calculated using Equation 3, as under:
322

$$f_{iso} = \frac{1}{2\pi}\sqrt{\frac{E_i \times A}{t_i \times m_{st}}} = \frac{1}{2\pi}\sqrt{\frac{40000 \times 16}{0.09 \times 148100}} = 3.5 \text{ Hz} \quad (5)$$

323 The described prototype was modeled both numerically and physically to achieve two main
324 objectives: confirming the effectiveness of layered foundations in a real-world situation and
325 validating the numerical modeling approach employed in this research.
326

4.1. Physical modeling of the prototype

Physical modeling involves creating a scaled-down version of a large, complex structure, known as a "prototype," while preserving the same physical characteristics and interactions with the environment (Harris and Sabnis, 1999). This method is used to replicate the behavior of the prototype under relevant loading and boundary conditions. A successful physical model must be designed, loaded, and interpreted based on similitude requirements that establish the relationship between the model and the prototype (Harris and Sabnis, 1999). In laboratory settings, physical modeling under 1-g conditions is particularly useful for studying railway-induced vibrations (Haghighi et al., 2023, 2024; W Yang et al., 2019; Yang et al., 2018).

To achieve the research objectives, a suitable physical model under 1-g conditions was developed. This approach has previously been utilized to analyze the impact of foundation geometry on building vibrations and to assess the effects of soil-structure interactions on the performance of isolation systems (Haghighi et al., 2023; Mousavi-Rahimi et al., 2022). Here, we enhance this model to evaluate the performance of a layered foundation.

Similitude requirements, which govern the dynamic relationships between the model and prototype, depend on the geometric and material properties of the prototype and the type of loading. Railway-induced vibrations typically produce small shear strains, allowing material behavior to be considered linearly elastic (Akbarov et al., 2018; Chen, 2015; Ling et al., 2019; Sun et al., 2015). Nine critical physical parameters are involved: geometry size (l), force (F), elastic modulus (E), Poisson's ratio (ν), mass density (ρ), displacement (δ), stress (σ), frequency (f), and gravity (g) (Harris & Sabnis, 1999). Scale factors are derived by equating the π terms in the model and prototype. The scale factor $S_i = S_p/S_m$ is defined for each quantity i, with subscripts p and m denoting prototype and model, respectively. Under 1-g conditions, the gravity similitude law ensures identical gravitational acceleration for both the model and prototype (S_g=1), known as the Cauchy condition. This condition requires that S_E equals S_ρ times S_l. Moreover, the mass density of soil is approximately the same in both the prototype and model (Yang et al., 2018, 2019), necessitating that S_ρ equals one (S_ρ=1). Consequently, all scaling factors are derived in terms of the geometric scaling factor (S_l=S), as shown in Table 4. Choosing a geometric scaling factor between 10 and 30, as recommended by Yang et al. (2018, 2019), the scale factor of 20 was selected in this study to balance cost and accuracy.

Table 4. Scaling factors for elastic vibrations (adapted from Haghighi et al., 2023)

Properties	Quantity	Symbol	Scale factors
Geometry	Length	*L*	$S_l = S = 20$
Dynamic response	Frequency	F	$1/\sqrt{S}$
	Time	T	$\sqrt{S}$
	Displacement	δ	*S*
	Velocity	V	$\sqrt{S}$
	Stress	σ	*S*
Loading	Force	*F*	S^3
	Gravity	*G*	*1*
Material	Density	*P*	*1*
	Young's modulus	*E*	*S*
	Poisson's ratio	*N*	*1*

Achieving perfect similarity (i.e., "true" modeling) between the model and prototype is challenging, especially in dynamic systems with multiple material types (e.g., soil-structure interaction). By focusing on first-order effects and neglecting some second-order effects, an "adequate" model can often accurately predict prototype behavior (Harris & Sabnis, 1999). In this regard, the building floor's natural frequency is a crucial factor influencing vertical vibration response (Allen, 1999), which should be equal between the true and adequate models. To account for soil-structure interaction, the building's total mass and the foundation-ground interfaces should also match between the models.

Simulations in ABACUS determined the prototype floor's natural frequencies to be 10 to 11 Hz. Scaling laws indicated that the model floor's frequencies should be about 45 to 50 Hz (S_f=1/√20), and the model's total mass should be approximately 18.5 kg (S_F=20^3). To meet these conditions, a building model (see Figure 9) was constructed using steel, comprising thin steel plates as floors, rebars as columns, and thick plates as foundations. Hence, all members of the adequate building model have a Young's modulus of 200 GPa, a Poisson's ratio of 0.3, and a density of 7850 kg/m³. Through trial and error and numerical simulations, the required mass and natural frequency were achieved, resulting in floor frequencies around 46-48 Hz. The floors have dimensions of 300 × 300 × 1 mm and a mass of 3.55 kg. The columns have a diameter of 10 mm and a mass of 2.38 kg. The

foundations measure 100 × 100 × 40 mm and have a mass of 12.56 kg. Altogether, the total mass of the model is 18.50 kg, meeting the scaling laws.

To simulate three-dimensional wave propagation in soil, we built a rectangular steel container measuring 200×100×80 cm, as shown in Figure 9. To minimize wave reflections from the container's rigid boundaries, 5 cm thick foam layers were installed on the inner walls, based on practical guidelines (Lombardi et al., 2015). Dynamic testing confirmed these foam layers effectively absorbed wave reflections (Haghighi et al., 2024). For the soil medium, Firuzkuh's uniformly graded (SP) sand was used, known for its consistency in geotechnical studies (Esmaeili & Khajehei 2016, Haghighi et al. 2023). This type of poorly-graded sand, characterized by a particle size range of 0.4 to 1 mm, was layered in 10 cm increments and compacted to maintain a density of 1570 kg/m³. The container was filled to a depth of 70 cm, representing a bedrock located at a depth of 14 meters. The soil model features a Poisson's ratio of 0.3 and a shear wave velocity of 132 m/s (Esmaeili and Khajehei, 2016; Mousavi-Rahimi et al., 2022), equivalent to 590 m/s in the prototype.

For the two isolation scenarios, a layer of polystyrene foam, measuring 10×10 cm and possessing a dynamic Young's modulus of 112 kPa, was utilized. Based on scaling laws, the isolation frequency in both isolation states should be around 16 Hz ($S_f = 1/\sqrt{20}$). The isolator layer's thickness was calculated to be 2.4 cm for a single layer scenario, while three 0.8 cm thick layers were used in the multi-layered scenario.

To perform the experiments, an impulsive load with an amplitude of about 18-20 N ($S_F = 20^3$) was applied at a distance of 100cm ($S_l = 20$) the building's center. The experiments utilized a variety of equipment including a PC, shaker, amplifier, data logger, and accelerometer. The accelerometer had a capacity of 500 m/s² within a frequency range of 1–5000 Hz, which covered the desired vibration range. To achieve maximum measurement precision, the sampling frequency was arranged to 1280 Hz. Furthermore, frequencies exceeding 312 Hz were removed from the measured data using an 8th-order low-pass digital filter of the MATLAB signal processing toolbox. Figure 9 provides a detailed view of the test instrumentation setup and different isolation configurations.

(a) instrumentation and test setup

(b) isolated building with single under foundation isolator

(c) isolated building with layered under foundation isolator.

Figure 9. Details of the physical model

4.2. Numerical modeling of the prototype

A 3D numerical model combining finite and infinite elements was created in ABAQUS to analyze the building, its isolators, and the underneath soil. As depicted in Figure 10, 4-node linear shell elements of S4 were used to represent the building's slabs, while solid elements of C3D8 (8-

node cubic 3-dimensional) were employed for the other components of the building, isolators, and the near-field underneath soil. To simulate the infinite expanse of the far-field soil and avoid wave reflections at the model's boundaries, 8-node cubic infinite 3-dimensional elements of CIN3D8 were incorporated (Systèmes, 2014; Zhang et al., 2019). The finite domain was designed to be 40 meters in both length and width, ensuring adequate space for the entire model configuration.

The depth of the finite domain was fixed at 14 m to represent the bedrock, aligning with the soil depth used in physical modeling. All material properties of the prototype were incorporated into the numerical model. Material damping was modeled using Rayleigh damping, which is particularly effective for time-domain analysis (Chopra, 1995). In this approach, the damping matrix is a linear combination of the mass and stiffness matrices. To simulate the dynamic response, an impulsive load with an amplitude of 150 kN (Equation 1) was implemented to the soil surface at a point 20 meters away from the center of the building. The resulting responses were measured at the middle of the first floor to assess the effectiveness of the isolation system.

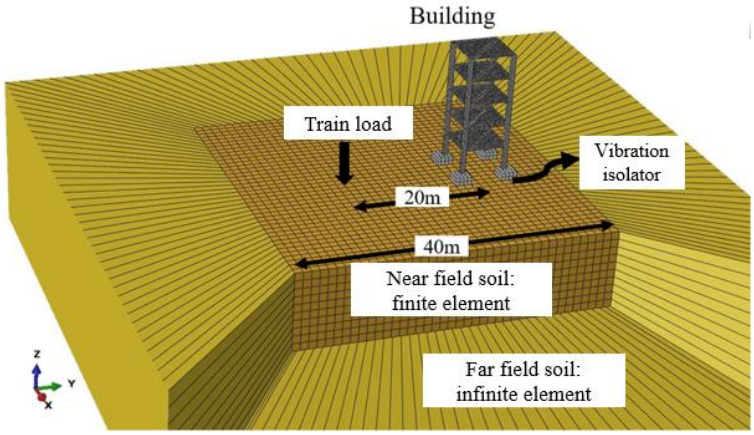

Figure 10. Geometry of the 3D finite/infinite numerical model.

4.3. Results of the physical and numerical models

The dynamic vertical responses at the midpoint of the first floor were measured for both experimental and 3D numerical models under isolated and unisolated conditions. The root mean square (RMS) values for the unisolated states were 0.066 mm/s for the physical model and 0.072 mm/s for the numerical model. In the single-layer isolated state, the RMS values decreased to 0.015

mm/s for the physical model and 0.017 mm/s for the numerical model, while the three-layer isolated state yielded RMS values of 0.019 mm/s and 0.021 mm/s, respectively.

The close agreement between the physical and numerical models, with differences under 10%, validates the employed numerical approach, ensuring reliability in predicting dynamic responses of a soil-structure interaction problem. Both isolation techniques significantly reduced vibrations, with single-layer isolators reducing levels by 12.5 dB and three-layer isolators by 10.7 dB, demonstrating their efficacy in mitigating train-induced vibrations. Although the single-layer isolators performed marginally better by 1.8 dB, the minimal difference suggests that multi-layer isolators with equivalent total rubber thickness are a practical alternative when the rubber mat's bearing capacity is a constraint.

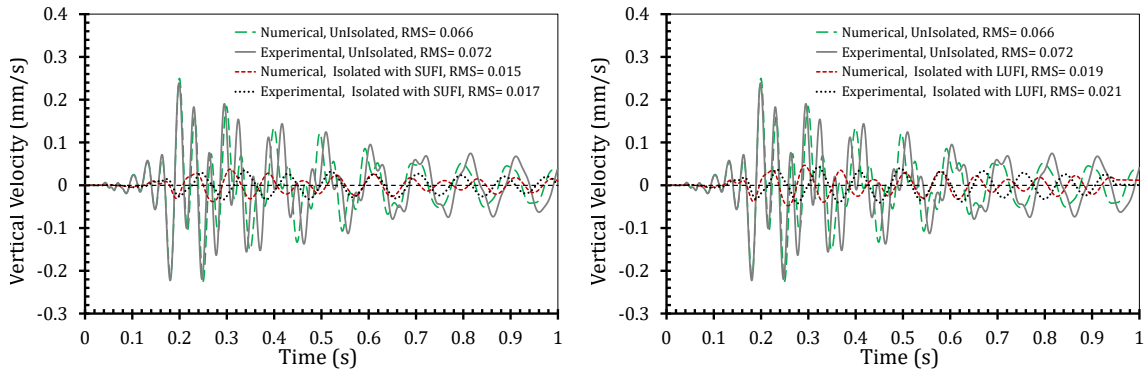

Figure 11. Comparison of numerical and physical model responses at the middle point of the first floor (in prototype scale): (a) unisolated building isolated building and isolated building with single under foundation isolator and (b) unisolated building isolated building and isolated building with layered under foundation isolator.

5. Conclusion

Performance of layered foundations in reducing railway-induced vibrations was thoroughly evaluated using both numerical and physical models. The study investigated various configurations of Single Under Foundation Isolators (SUFI) and Layered Under Foundation Isolators (LUFI) to determine their effectiveness in mitigating vibrations. The findings indicate that increasing the

isolation frequency from 3 Hz to 12 Hz results in a significant reduction in isolation efficiency, with an average decrease of about 20 dB in both horizontal and vertical directions. This highlights the importance of maintaining lower isolation frequencies for effective vibration mitigation. Additionally, the stiffness of the underlying soil, characterized by the soil shear wave velocity, significantly impacts the isolators' performance, with stiffer soils enhancing the effectiveness of the isolation systems. The natural frequency of the building's floor also plays a crucial role in the effectiveness of the isolators. Buildings with higher natural frequencies exhibited different trends in isolation efficiency compared to those with lower frequencies, underscoring the complex interaction between soil and structure.

When comparing different types of isolators, single-layer isolators (SUFI-t) generally outperformed 2-layer and 4-layer isolators when the total thickness of the isolator was constant (2LUFI-t and 4LUFI-t). This suggests that a single-layer configuration provides better vibration isolation due to more uniform deformation and energy dissipation. In the scenarios where each isolator layer had a rubber thickness of t, multi-layer isolators significantly improved the performance compared to single-layer isolators. Specifically, the 4LUFI-4t isolator outperformed the 2LUFI-2t and SUFI-t isolators, demonstrating that adding more layers enhances the isolator's ability to dampen vibrations effectively. This improvement is attributed to the increased flexibility and improved damping capacity provided by additional layers, allowing the isolator to better absorb and mitigate vibrational energy. These results emphasize the advantage of multi-layered isolators in the applications where superior vibration isolation is crucial.

The proposed isolation method's effectiveness in a real-world setting was examined by creating both a 3D numerical model and a scaled-down laboratory model of a building near a railway track. In this regard, the performance of single resilient layers and three-layer foundations in mitigating ground-borne vibrations were compared. Both isolation techniques effectively reduced vibrations: single-layer isolators cut levels by 12.5 dB, while three-layer isolators reduced them by 10.7 dB. Single-layer isolators were slightly more effective, by 1.8 dB, but the difference is minor. Thus, multi-layer isolators with the same total rubber thickness are a viable option when bearing capacity is a concern. The accuracy of the numerical approach was also validated by comparing its results to those from the laboratory model, revealing differences of less than 10%.

Overall, the study highlights that multi-layered isolators can offer superior performance in reducing railway-induced vibrations, especially in scenarios where maintaining low isolation

frequencies is critical while bearing capacity is constrained. These findings contribute to the development of more effective strategies for mitigating vibrations in buildings located near railway tracks, enhancing the comfort and safety of building occupants.

AI ethics statement

The authors employed ChatGPT to enhance the language and readability of this manuscript. After using this tool, the authors reviewed and edited the content afterward and take full responsibility for the final version.

Declaration of competing interest

The authors declare that they have no known competing financial interests or personal relationships that could have appeared to influence the work reported in this paper.

References

Bachmann H and Ammann W (1987) *Vibrations in Structures: Induced by Man and Machines*. Iabse.

Celebi E and Göktepe F (2012) Non-linear 2-D FE analysis for the assessment of isolation performance of wave impeding barrier in reduction of railway-induced surface waves. *Construction and Building Materials* **36**. Elsevier: 1–13.

Cheng Z, Shi Z, Palermo A, et al. (2020) Seismic vibrations attenuation via damped layered periodic foundations. *Engineering Structures* **211**. Elsevier: 110427.

Chopra AK (1995) *Dynamics of Structures: Theory and Applications to Earthquake Engineering*. Prentice Hall.

Dassault Systèmes S (2014) ABAQUS 6.14. *Theory and User's Manuals*.

Engineers A (2010) Minimum design loads for buildings and other structures. *ASCE 7* 10.

Esmaeili M and Khajehei H (2016) Mechanical behavior of embankments overlying on loose subgrade stabilized by deep mixed columns. *Journal of Rock Mechanics and Geotechnical Engineering* **8**(5). Elsevier: 651–659.

Farahani MV, Sadeghi J, Jahromi SG, et al. (2023) Modal based method to predict subway train-induced

vibration in buildings. In: *Structures*, 2023, pp. 557–572. Elsevier.

Haghighi E, Pooshideh SM and Ghadami A (2023) Building isolation against train-induced vibrations considering the effects of soil and structure: A numerical and experimental study. *Soil Dynamics and Earthquake Engineering* **175**. Elsevier: 108251.

Haghighi E, Sadeghi J and Esmaeili M (2024) Experimental investigation on the effectiveness of under-foundation isolator against train-induced vibrations considering foundation type. *Structural Engineering and Mechanics* **89**(2). TECHNO-PRESS PO BOX 33, YUSEONG, DAEJEON 305-600, SOUTH KOREA: 121–133.

Hanson CE, Towers DA and Meister LD (2006) *Transit noise and vibration impact assessment*.

Harris HG and Sabnis G (1999) *Structural Modeling and Experimental Techniques*. CRC press.

Isolgomma (2024) No Title. Available at: https://www.isolgomma.com/.

Kelly JM and Konstantinidis D (2011) *Mechanics of Rubber Bearings for Seismic and Vibration Isolation*. John Wiley & Sons.

Khajehdezfuly A, Shiraz AA and Sadeghi J (2023) Assessment of vibrations caused by simultaneous passage of road and railway vehicles. *Applied Acoustics* **211**. Elsevier: 109510.

Kouroussis G, Conti C and Verlinden O (2013) Investigating the influence of soil properties on railway traffic vibration using a numerical model. *Vehicle System Dynamics* **51**(3). Taylor & Francis: 421–442.

Lei X and Jiang C (2016) Analysis of vibration reduction effect of steel spring floating slab track with finite elements. *Journal of Vibration and Control* **22**(6). SAGE Publications Sage UK: London, England: 1462–1471.

Li M, Ma M, Liu W, et al. (2019) Influence of static preload on vibration reduction effect of floating slab tracks. *Journal of Vibration and Control* **25**(6). SAGE Publications Sage UK: London, England: 1148–1163.

Lombardi D, Bhattacharya S, Scarpa F, et al. (2015) Dynamic response of a geotechnical rigid model container with absorbing boundaries. *Soil Dynamics and Earthquake Engineering* **69**. Elsevier: 46–56.

Mousavi-Rahimi M, Zakeri JA and Esmaeili M (2022) Effect of Foundation Geometry and Structural Properties of Buildings on Railway-Induced Vibration: An Experimental Modeling. *Buildings* **12**(5). Multidisciplinary Digital Publishing Institute: 604.

Newland DE (2013) *Mechanical Vibration Analysis and Computation*. Courier Corporation.

Newland DE and Hunt HEM (1991) Isolation of buildings from ground vibration: a review of recent progress. *Proceedings of the Institution of Mechanical Engineers, Part C: Mechanical Engineering Science* **205**(1). SAGE Publications Sage UK: London, England: 39–52.

Pan P, Shen S, Shen Z, et al. (2018) Experimental investigation on the effectiveness of laminated rubber bearings to isolate metro generated vibration. *Measurement* **122**. Elsevier: 554–562.

Pu X and Shi Z (2020) Broadband surface wave attenuation in periodic trench barriers. *Journal of Sound and Vibration* 468. Elsevier: 115130.

Pu X, Shi Z and Xiang H (2018) Feasibility of ambient vibration screening by periodic geofoam-filled trenches. *Soil Dynamics and Earthquake Engineering* **104**. Elsevier: 228–235.

Ribes-Llario F, Marzal S, Zamorano C, et al. (2017) Numerical modelling of building vibrations due to railway traffic: Analysis of the mitigation capacity of a wave barrier. *Shock and Vibration* 2017. Hindawi.

Sadeghi J and Esmaeili MH (2017) Safe distance of cultural and historical buildings from subway lines. *Soil Dynamics and Earthquake Engineering* **96**. Elsevier: 89–103.

Sadeghi J and Vasheghani M (2021) Safety of buildings against train induced structure borne noise. *Building and Environment* **197**. Elsevier: 107784.

Sadeghi J and Vasheghani M (2022) Improvement of current codes in design of concrete frame buildings: Incorporating train-induced structure borne noise. *Journal of Building Engineering* **58**. Elsevier: 104955.

Sadeghi J, Haghighi E and Esmaeili M (2021) Performance of under foundation shock mat in reduction of railway - induced vibrations. *Structural Engineering and Mechanics* **4**: 425–437.

Sadeghi J, Haghighi E and Esmaeili M (2022) Effectiveness of grouted layer in the mitigation of subway-induced vibrations. *Proceedings of the Institution of Mechanical Engineers, Part F: Journal of Rail and Rapid Transit*. SAGE Publications Sage UK: London, England: 09544097221089417.

Sadeghi J, Vasheghani M and Khajehdezfuly A (2023) Propagation of structure-borne noise in building adjacent to subway lines. *Construction and Building Materials* **401**. Elsevier: 132765.

Sadeghi J, Toloukian A and Shafieyoon Y (2024) Metro-induced vibration attenuation using rubberized concrete slab track. *Construction and Building Materials* **435**. Elsevier: 136754.

Sheng T, Shi W, Shan J, et al. (2020) Base isolation of buildings for subway-induced environmental vibration: Field experiments and a semi-analytical prediction model. *The Structural Design of Tall and Special Buildings*. Wiley Online Library: e1798.

Soares PJ, Arcos R, Costa PA, et al. (2024) Experimental and numerical study of a base-isolated building subjected to vibrations induced by railway traffic. *Engineering Structures* **316**. Elsevier: 118467.

Sol-Sánchez M, Moreno-Navarro F and Rubio-Gámez MC (2015) The use of elastic elements in railway tracks: A state of the art review. *Construction and building materials* **75**. Elsevier: 293–305.

Standard I (2010) Mechanical vibration and shock — Evaluation of human exposure to whole-body vibration. *International Organization for Standardization* **26**(1): 2010–2631. Available at: www.iso.org.

Standard I and ISO B (2005) Mechanical vibration—ground-borne noise and vibration arising from rail systems. *ISO 14837* 1.

Standard ISO (1989) ISO2631/2: Mechanical vibration and shock-evaluation of human exposure to whole body vibration——Part2: Continuous and shock induced vibration in buildings (1—80 Hz). Washington DC ISO Standard.

Systèmes D (2014) Abaqus 6.14: Abaqus/CAE User's Guide. *http://130.149* 89(2080): v6.

T. L. Edirisinghe and J. P. Talbot (2022) Some observations on the transmission of ground-borne vibration into base-isolated buildings. Leuven, Belgium: ISMA 2022: 30th International Conference on Noise and Vibration Engineering and USD.

Talbot JP (2002) On the performance of base-isolated buildings: a generic model. University of Cambridge.

Talbot JP (2007) Base isolation of buildings for control of ground-borne vibration. John Wiley & Sons.

Talbot JP, Hamad WI and Hunt HEM (2014) Base-isolated buildings and the added-mass effect. In: *Proceedings of ISMA 2014: International Conference on Noise and Vibration Engineering*, 2014.

Towhata I (2008) *Geotechnical Earthquake Engineering*. Springer Science & Business Media.

Toygar O and Ulgen D (2021) A full-scale field study on mitigation of environmental ground vibrations by using open trenches. *Building and Environment* **203**. Elsevier: 108070.

Xu Q, Xiao Z, Liu T, et al. (2015) Comparison of 2D and 3D prediction models for environmental vibration induced by underground railway with two types of tracks. *Computers and Geotechnics* **68**. Elsevier: 169–183.

595 Yang J, Zhu S, Zhai W, et al. (2019) Prediction and mitigation of train-induced vibrations of large-scale
596 building constructed on subway tunnel. *Science of the Total Environment* 668. Elsevier: 485–499.

597 Yang W, Cui G, Xu Z, et al. (2018) An experimental study of ground-borne vibration from shield tunnels.
598 *Tunnelling and Underground Space Technology* **71**. Elsevier: 244–252.

599 Yang W, Zhang C, Liu D, et al. (2019) The effect of cross-sectional shape on the dynamic response of tunnels
600 under train induced vibration loads. *Tunnelling and Underground Space Technology* **90**. Elsevier: 231–
601 238.

602 Yang Y-B and Hung HH (2009) *Wave Propagation for Train-Induced Vibrations: A Finite/Infinite Element*
603 *Approach*. World scientific.

604 Yang YB, Liang X, Hung H-H, et al. (2017) Comparative study of 2D and 2.5 D responses of long underground
605 tunnels to moving train loads. *Soil Dynamics and Earthquake Engineering* **97**. Elsevier: 86–100.

606 Yuan X, Zhu S, Xu L, et al. (2020) Investigation of the vibration isolation performance of floating slab track
607 with rubber bearings using a stochastic fractional derivative model. *Proceedings of the Institution of*
608 *Mechanical Engineers, Part F: Journal of Rail and Rapid Transit* **234**(9). SAGE Publications Sage UK:
609 London, England: 992–1004.

610 Zakeri J, Esmaeili M and Mousavi-Rahimi M (2020) Effect of foundation shape and properties of the adjacent
611 buildings on the railway-induced vibrations. *Asian Journal of Civil Engineering* **21**(7): 1095–1108. DOI:
612 10.1007/s42107-020-00264-w.

613 Zhang W, Seylabi EE and Taciroglu E (2019) An ABAQUS toolbox for soil-structure interaction analysis.
614 *Computers and Geotechnics* **114**. Elsevier: 103143.

615 Zhang X, Zhou S, He C, et al. (2021) Experimental investigation on train-induced vibration of the ground
616 railway embankment and under-crossing subway tunnels. *Transportation Geotechnics* **26**. Elsevier:
617 100422.

618 Zhao C, Shi D, Zheng J, et al. (2022) New floating slab track isolator for vibration reduction using particle
619 damping vibration absorption and bandgap vibration resistance. *Construction and Building Materials*
620 **336**. Elsevier: 127561.

621 Zhou F, Zhou Z and Ma Q (2022) Study on the vibration isolation performance of an open trench–wave
622 impedance block barrier using perfectly matched layer boundaries. *Journal of Vibration and Control*
623 **28**(3–4). SAGE Publications Sage UK: London, England: 329–338.